Contents lists available at ScienceDirect

Applied Catalysis B: Environmental

FT-IR study of the surface redox states on platinum-potassium-alumina catalysts

Tania Montanari [a,1], Roberto Matarrese [b], Nancy Artioli [b], Guido Busca [a,*]

[a] *Laboratorio di Chimica delle Superfici e Catalisi Industriale, Dipartimento di Ingegneria Chimica e di Processo, Università di Genova, Piazzale Kennedy 1, I-16129 Genova, Italy*
[b] *Dipartimento di Energia, Laboratory of Catalysis and Catalytic Processes and NEMAS, Centre of Excellence, Politecnico di Milano, P.za Leonardo Da Vinci 32, I-20133 Milano, Italy*

ARTICLE INFO

ABSTRACT

Pt–K/Al$_2$O$_3$ (Pt 1%; K 5.4% wt/wt) catalyst active for the simultaneous Diesel particulate oxidation and NO$_x$ reduction have been characterized in comparison with 1% Pt/Al$_2$O$_3$ catalyst. IR spectra of adsorbed CO at −140 °C and at room temperature allowed the detection of oxidized Pt centers and of their very strong oxidizing ability. TPD and IR spectra of adsorbed CO$_2$ allowed to characterize the basicity of the samples. The data indicate that Pt centers lie in close proximity of potassium oxide species generating basicity.

© 2011 Elsevier B.V. All rights reserved.

1. Introduction

Platinum/alumina based catalysts are largely used in industry for several reactions, such as hydrogenations and dehydrogenations. As examples, Pt/Al$_2$O$_3$ is used in the BenSat process to hydrogenate benzene to cyclohexane in gasoline fractions [1], in the Oleflex light paraffin dehydrogenation technology and in the Pacol long linear paraffin dehydrogenation technology, all from UOP [2]. Such catalysts may also contain alkalis and additional activator metals, such as Sn [3]. Pt/Al$_2$O$_3$ based catalysts are also applied to reactions where water acts as a reactant, like for water gas shift reaction for fuel cell applications [4], and act as of promising catalysts for dry reforming of methane [5].

Platinum/alumina represents also an important system for catalytic oxidation, like the SELECTOXO™ process for the preferential oxidation of CO in the presence of hydrogen (PROX) [6]. For this reaction K is reported to act as a promoter of Pt/Al$_2$O$_3$ [7]. Pt/Al$_2$O$_3$ based catalysts containing also base metals are patented for ammonia selective oxidation (SCO) to N$_2$ [8], and are used as VOC catalytic oxidation catalysts [9]. For this reaction potassium may act as a promoter as well [10].

Generally speaking, alkali ions are frequently added as dopants at the surface of metal catalysts to introduce basicity or to reduce acidity, and in catalysis "assisted by basicity" [11]. Potassium is frequently preferred to sodium possibly because of its larger ionic size that limits reactivity towards supports and the formation of bulk salts, as well as results in higher basicity.

Pt–K/Al$_2$O$_3$ sorbents-catalysts, typically containing ∼1 and 8% wt/wt of Pt and K have also been proposed for the "NO$_x$ storage-reduction" (NSR) reaction, a recent technology developed by Toyota in the early nineties [12,13] to reduce the NO$_x$ content in the exhaust gases of lean-burn gasoline engines. A further evolution of this technology is the DPNR (Diesel particulate-NO$_x$ reduction) process, for the simultaneous NO$_x$ and soot removal [14,15]. This catalytic system works alternatively in oxidizing (lean burn) condition (where Pt is supposed to catalyze the oxidation of NO to NO$_2$, favouring NO$_x$ storage and soot combustion) and in reducing conditions (where Pt is supposed to catalyze the reduction of adsorbed NO$_x$ to N$_2$). Potassium acts as the sorbent for NO$_x$ storage [16].

While most characterization studies concern reduced noble metal catalysts, much less is known about Pt/Al$_2$O$_3$ in oxidized or unreduced state. According to some of us [17], the location of Pt species on the alumina surface is "selective", substituting or exchanging the OH sites located on tetrahedral Al species, giving rise to isolated oxidized Pt ions, while they only perturb the OHs located over octahedral Al species. Quite in contrast with this, Kwak et al. proposed that bulk-like PtO layers form at the surface of γ-Al$_2$O$_3$ by interacting with pentacoordinated Al^{3+} species [18].

The IR spectroscopy of low temperature adsorption of CO is today a very popular technique for the characterization of solid sur-
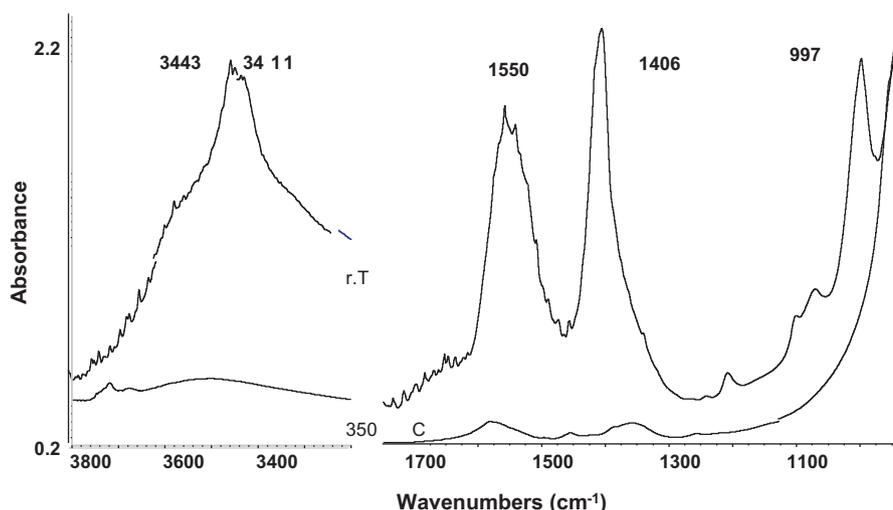
Fig. 1. FT-IR spectra of pure powder pressed disk of the Pt-K/Al$_2$O$_3$ sample after brief outgassing at r.t. and after activation at 350 °C.

faces, both of metallic and of oxide nature [19–21]. This is because CO, if adsorbed at low temperature (350–423 °C), is a very good and gentle probe for surface hydroxy-groups, cationic and metallic centers, with small or not surface perturbation nor reactivity. When dealing with noble-metal based oxidation catalysts, this technique allows the detection of oxidized ions, which is not always an easy matter [22–24].

In this paper we will summarize our data concerning IR spectroscopy of low temperature adsorption of CO on catalysts belonging to the Pt-K/Al$_2$O$_3$ system, with the aim to clarify the role of potassium in modifying the behavior of Pt/Al$_2$O$_3$ catalysts. This characterization study has been performed with and without previous reduction, just because Pt-K/Al$_2$O$_3$ catalysts work in oxidizing conditions when working as NO$_x$ traps as well as total oxidation catalysts, while they work in reducing conditions in the short step needed to reduce adsorbed NO$_x$.

2. Experimental

Pt-K/Al$_2$O$_3$ catalyst (Pt: ~1 wt.%, K: 5.4 wt.%) was obtained by impregnation in two sequential steps of a commercial γ-Al$_2$O$_3$ carrier (Versal 250 from UOP, surface area of 200 m^2/g and pore volume near 1 cm^3/g), as follows: the γ-Al$_2$O$_3$ powder was at first impregnated with a solution of Pt(NH$_3$)$_2$(NO$_2$)$_2$ (Strem Chemicals, 5% Pt in ammonium hydroxide) with an appropriate concentration so as to yield 1 wt.% Pt metal loading. After drying in air for 12 h at 80 °C and calcination at 500 °C for 5 h, the sample was impregnated with CH$_3$COOK (Sigma Aldrich, 99%) solution so as to yield a K content equal to 5.4 wt.%. After that, the sample was dried for 12 h at 80 °C and then calcined at 500 °C for 5 h (sample denoted as prepared, a.p. in the following). For comparative purposes, two reference binary systems, Pt/Al$_2$O$_3$ (Pt: 1 wt.%) and K/Al$_2$O$_3$ (K: 5.4 wt.%), were also prepared using the same precursors and procedures. The Pt dispersion on samples activated by heating in vacuo and subsequently in dry oxygen at 1096 °C and finally reduced in H$_2$ at 896 °C was estimated by hydrogen chemisorption to be 64.8% on Pt/Al$_2$O$_3$ and 71.7% on Pt-K/Al$_2$O$_3$.

IR skeletal studies have been performed using KBr pressed disks. For IR adsorption studies, pressed disks of the pure catalysts powders were activated "in situ" by using an infrared cell connected to a conventional gas manipulation/outgassing ramp. All catalysts were first submitted to a treatment in oxygen (200 Torr) at 350 °C, for 1 h, followed by evacuation at the same temperature before the adsorption experiments. In order to obtain the reduced catalysts,

after the mentioned evacuation, they were put in contact with a H$_2$ pressure (~400 Torr) at 350 °C, two cycles for 30 min, and successively outgassed at the same temperature. CO adsorption was performed at −140 °C by the introduction of a known dose of the gas (1 Torr) inside the low temperature infrared cell containing the previously activated wafers. IR spectra were collected evacuating at increasing temperatures between −140 °C and room temperature (r.t.). Spectra have been recorded in the same temperature range by a Nicolet Nexus FT instrument.

The thermal stability of carbonate species formed on K/Al$_2$O$_3$ and Pt–K/Al$_2$O$_3$ was analyzed by thermal decomposition in inert flow (temperature programmed desorption, TPD) in a flow-reactor apparatus consisting of a quartz tube reactor (7 mm i.d.) connected to a mass spectrometer (Omnistar 200, Pfeiffer Vacuum) and to a microGC (Agilent 3000A) for the on-line analysis of the outlet gases. For this purpose after CO$_2$ adsorption (3000 ppm v/v in flowing helium) at 100 °C the sample was then heated (10 °C/min) in He up to 500 °C. 60 mg of catalyst was used in each run, and the total gas flow was always set at 100 cm^3/min (at 0 °C and 1 atm). Before catalytic tests, the samples have been heated at 500 °C in He to remove any adsorbed species on the catalytic surface.

3. Results and discussion

3.1. Surface hydroxyl groups

The spectra of the pure powder pressed disks of both K/Al$_2$O$_3$ and Pt-K/Al$_2$O$_3$ samples before any activation treatment are very similar (see Fig. 1 for Pt-K/Al$_2$O$_3$) and show the strong bands of carbonate and hydroxide species with additional features at 3443, 3411, 1550, 1406, 997 cm^{-1}. The absence of evident scissoring mode of water suggests that this species is essentially an hydroxy-carbonate species. A similar spectrum was found previously for a 12% wt/wt K$_2$CO$_3$-Al$_2$O$_3$ catalyst [25]. Outgassing at 350 °C of both K/Al$_2$O$_3$ and Pt-K/Al$_2$O$_3$ samples causes the almost complete disappearance of these bands, suggesting that such species are decomposed with release of CO$_2$ and water. Both samples show, after activation at 350 °C, only weak bands in the region 1700–1200 cm^{-1} (see Fig. 1 for Pt-K/Al$_2$O$_3$), due to surface impurities (carbonates and/or carboxylates).

As expected, all samples show bands in the region 3800–3400 cm^{-1} (Fig. 2), due to OH stretchings of surface hydroxy groups. In the case of alumina support we find maxima at 3726, 3675 and 3575 cm^{-1}, with additional shoulders at
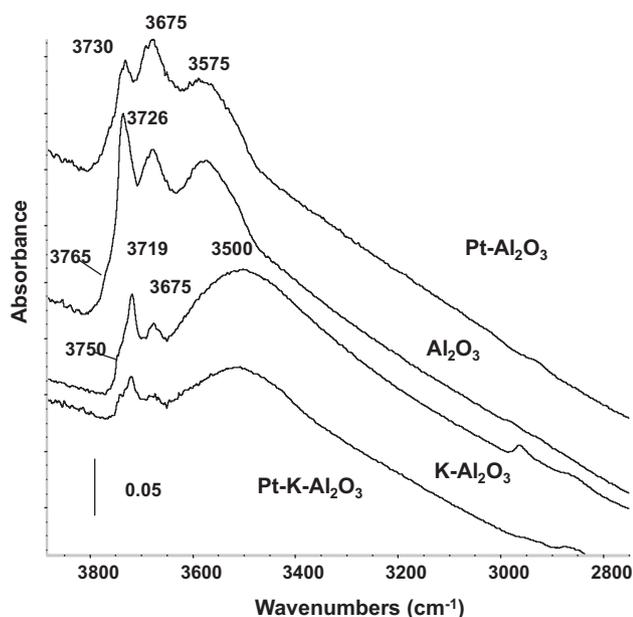
Fig. 2. FT-IR spectra of pure powder pressed disks of the catalysts after activation at 350 °C (OH stretching region).

$3765 \, cm^{-1}$ and near $3500 \, cm^{-1}$. This spectrum is quite typical for $\gamma\text{-}Al_2O_3$ samples outgassed at medium temperature. Our previous studies [26] suggested that the higher frequency component at $3765 \, cm^{-1}$ is due to terminal hydroxy-groups bonded to Al ions in a tetrahedral-like environment, the splitting being associated to vacancies with respect to the spinel-type composition. The band at $3725 \, cm^{-1}$, instead, is present also at the surface of $\alpha\text{-}Al_2O_3$ and of stoichiometric spinels, and is consequently likely due to terminal OHs on Al ions in octahedral-like environment. The additional

components at 3675 and $3575 \, cm^{-1}$ are assigned to bridging and triply bridging OHs, respectively.

The Pt/Al_2O_3 sample shows, in these conditions, a quite similar spectrum with respect to the support, but the intense band at $3725 \, cm^{-1}$ on alumina is shifted a bit upwards and significantly weakened in intensity. A similar result was observed previously with respect to another Pt/Al_2O_3 catalyst [17].

The K/Al_2O_3 sample shows the lower frequency feature broadened and shifted to near $3500 \, cm^{-1}$, while all higher frequency features are definitely weaker than on the support. This is likely due to partial K^+ for H^+ cationic exchange. Here we find very sharp a band at $3719 \, cm^{-1}$ with a shoulder at $3750 \, cm^{-1}$. The position of this band is similar to that reported previously for different $K\text{-}Al_2O_3$ samples ($3715 \, cm^{-1}$ [27]) and for a 12% wt/wt $K_2CO_3\text{-}Al_2O_3$ catalyst ($3710 \, cm^{-1}$ [25]). On titania, K doping causes the formation of a band at $3720\text{–}3712 \, cm^{-1}$ [28]. The spectrum of the $Pt\text{-}K/Al_2O_3$ sample is very similar to that of K/Al_2O_3.

3.2. IR study of the adsorption of carbon monoxide

In Fig. 3 the spectra of carbon monoxide adsorbed on the support $\gamma\text{-}Al_2O_3$ (upper spectra, A–C) as well as on the K/Al_2O_3 (lower spectra, D–F) are reported and compared. In the left parts of the figure the spectra are recorded during adsorption after admission of CO into the cell, in the right section the spectra recorded during outgassing upon warming. At the highest coverages the main maximum on alumina is at $2153 \, cm^{-1}$. Looking at the OH stretching region (see the insert C in Fig. 3) it is evident that this band is associated to the H-bonding of CO with surface hydroxy-groups. Upon this interaction, the band at $3725 \, cm^{-1}$ is involved partially, being shifted in part to near $3600 \, cm^{-1}$. The component at $3675 \, cm^{-1}$ seems almost not involved, being still evident. The shift of the OH stretching band is, consequently, in the range $\Delta\nu OH \sim 125 \, cm^{-1}$, which allows to denote the alumina's OH as medium strength Brønsted acid sites. Thus the band at $2153 \, cm^{-1}$ is attributed to CO H-bonded on the terminal hydroxy groups of
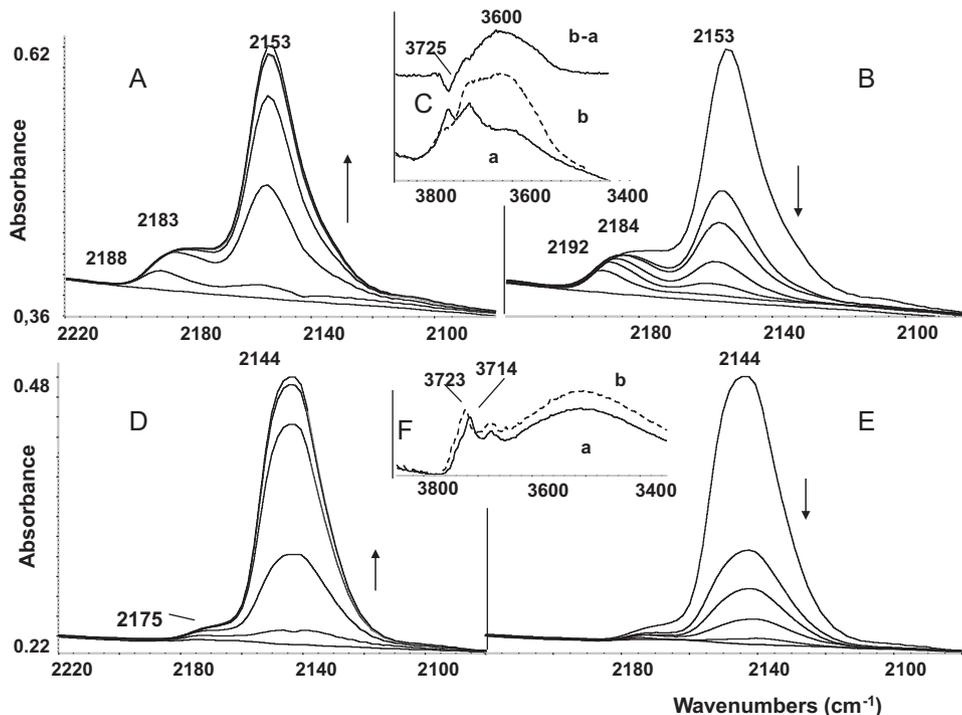

Fig. 3. FT-IR spectra of Al_2O_3 (A–C) and of K/Al_2O_3 (D–F) at −140 °C after admission of CO gas into the cell until saturation (A and D) and upon outgassing at increasing temperatures from −140 to −90 °C (B and E). In the inserts C and E: OH stretching region of the samples at −140 °C before (a) and after (b) saturation with CO, and the corresponding difference (after saturation − before saturation).
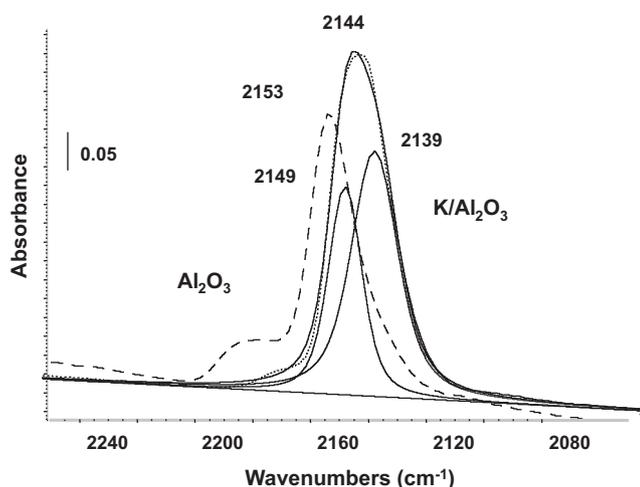
Fig. 4. FT-IR spectra of CO adsorbed (at saturation at −140 °C) on Al$_2$O$_3$ (dashed line), K/Al$_2$O$_3$ (pointed line), and the deconvolution of the spectrum recorded on K/Al$_2$O$_3$ (light full lines peak deconvolution; heavy full line sum).

Fig. 5. FT-IR spectra of unreduced Pt/Al$_2$O$_3$ at −140 °C after admission of CO gas into the cell until saturation (A) and upon outgassing at increasing temperatures from −140 to −90 °C (B). In the inserts: (C) OH stretching region of unreduced Pt/Al$_2$O$_3$ at −140 °C before and after saturation with CO, and the corresponding difference (after saturation − before saturation); (D) the spectrum of CO adsorbed just after admission (lowest coverage); (E) the spectrum of residual CO adsorbed after outgassing at −90 °C.

alumina on Al ions in octahedral-like environment. In agreement with this assignment, this band disappears fast upon outgassing at low temperature.

A weaker feature, more resistant to outgassing, is observed at higher frequencies, shifting from near 2180 cm^{-1} to 2192 cm^{-1} upon outgassing. It does not correspond to any perturbation of the νOH bands. It is assigned to CO species interacting with Lewis acidic Al^{3+} cations. The shift with respect to νCO of gas or liquid CO is relatively weak, and this shows that after outgassing at 350 °C the strongest Lewis sites of alumina are still not produced, being the surface still in a highly hydroxylated state.

In the low section of Fig. 3 the spectra of carbon monoxide adsorbed on sample K/Al$_2$O$_3$ are reported. At the highest coverages the main maximum is at 2144 cm^{-1}, i.e. definitely lower than in the case of pure alumina. The height of the band is similar in the two cases. However, the shape of the band is different, being definitely broader for K/Al$_2$O$_3$. A deconvolution of this spectrum is shown in Fig. 4, where it is superimposed to the band observed on alumina. At least two components are evident in the deconvolution of the spectrum observed on K/Al$_2$O$_3$, located at 2149 cm^{-1}, less intense, and at 2139 cm^{-1}, more intense. Looking at the OH stretching region (compare inserts C and d in Fig. 3) we note here that the spectrum is, in this region, less perturbed. The sharp band at 3714 cm^{-1} is shifted up to 3723 cm^{-1}, certainly due to a secondary interaction. No H-bonding with CO is found in this case. Our data support the assignment of this band to CO adsorbed on two different families of K$^+$ ions. In fact, the position of this band is at slightly lower frequency than that found on K-zeolites (2170–2150 cm^{-1} [29]) where K ions are bonded to a less basic structure. Low temperature CO adsorption on K$_2$O–TiO$_2$ was reported previously to produce a band at 2148 cm^{-1} [28]. At least two different families of potassium ions are formed, differing in their Lewis acidity.

The data reported here show that, over this heavily K-doped alumina, the surface hydroxy groups have totally lost their Brønsted acidity and K$^+$ ions display very weak Lewis acidity, although they appear to be well exposed at the surface.

The weaker feature, more resistant to outgassing, found near 2175 cm^{-1}, is assigned to CO species interacting with residual Lewis acidic Al^{3+} cations. The position of this band, shifted downwards with respect to pure alumina, and the intensity, definitely weaker than on pure alumina (compare Fig. 3, A and B, with Fig. 3, C and D, and see Fig. 4), show that potassium species cover the surface, mainly interacting with the strongest Lewis sites. Thus only part
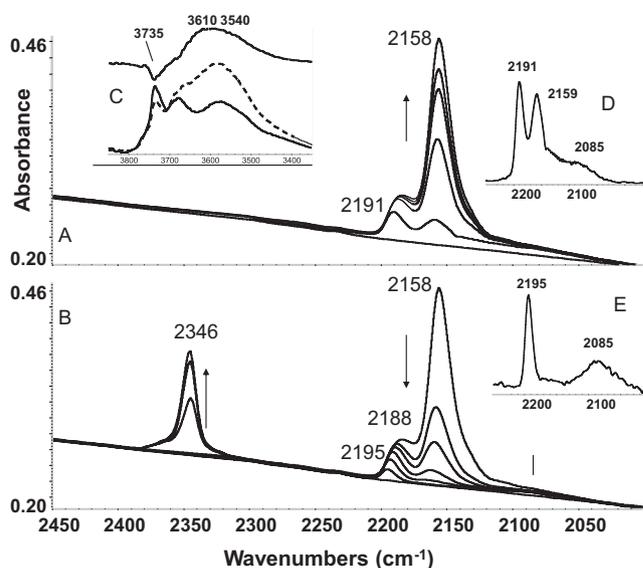
of weaker Lewis sites of alumina are residual, in small amounts. This result is quite similar to that reported previously for K-doped alumina using pyridine and nitrile as the probes [27].

In Fig. 5 the spectra of carbon monoxide adsorbed on the Pt/Al$_2$O$_3$ catalyst are reported. In the upper part of the figure (A) the spectra are recorded during adsorption after admission of CO into the cell, in the lower section (B) the spectra recorded during outgassing upon warming. At the highest coverages the main maximum is at 2158 cm^{-1}, i.e. 5 cm^{-1} higher than on pure alumina. Looking at the OH stretching region (see the insert C in Fig. 5) it is evident that this band is associated to the H-bonding of CO with surface hydroxy-groups. Upon this interaction, the band at 3735 cm^{-1} is involved partially, being shifted in part to near 3600 cm^{-1}. Actually, we find two unresolved components at 3610 and 3540 cm^{-1}. The component at 3675 cm^{-1} seems again almost not involved, being still evident. The shift of the OH stretching band is, consequently, in the range $\Delta\nu$OH $\sim$125–200 cm^{-1}. In any case it seems that the Brønsted strength of alumina's OH is not much perturbed by addition of Pt, being perhaps a little strengthened, in agreement also to the slight shift up of the corresponding νCO.

On the other hand, a weak tail at lower frequency is observed on the spectrum recorded during adsorption, which is more clearly evident upon desorption as a single band centred at 2085 cm^{-1}. This absorption is typical for terminal carbonyls on Pt° particles whose average size is of the order of few nanometers [30]. Upon outgassing and warming, a band also grows at 2346 cm^{-1}, due to OCO asymmetric stretching of adsorbed CO$_2$. This reactivity is not found on pure alumina. This shows that unreduced Pt centers exist and are able to oxidize CO to CO$_2$. Quite obviously, the second oxygen atom comes from the oxide species balancing Pt cations.

Also on Pt/Al$_2$O$_3$ a band more resistant to outgassing is observed at higher frequencies, shifting from near 2188 cm^{-1} to 2195 cm^{-1} upon outgassing. This absorption is in the region of bands typically assigned to CO species interacting with Lewis acidic Al^{3+} cations.

The same experiment has been performed with pre-reduced Pt/Al$_2$O$_3$, as shown in Fig. 6. In this case the main band is in the same position than on pure alumina (2153 cm^{-1}). The formation of CO$_2$ is much lower, confirming that our mild reduction pre-treatment
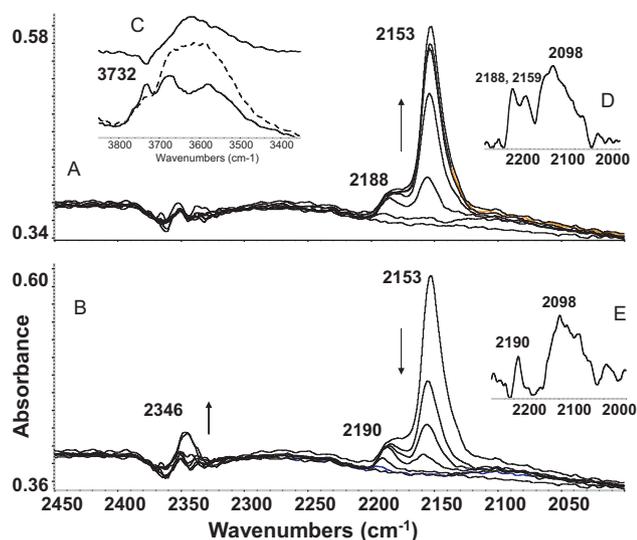
Fig. 6. FT-IR spectra of prereduced Pt/Al_2O_3 at $-140\,^\circ C$ after admission of CO gas into the cell until saturation (A) and upon outgassing at increasing temperatures from -140 to $-90\,^\circ C$ (B). In the inserts: (C) OH stretching region of prereduced Pt/Al_2O_3 at $-140\,^\circ C$ before and after saturation with CO, and the corresponding difference (after saturation – before saturation); (D) the spectrum of CO adsorbed just after admission (lowest coverage); (E) the spectrum of residual CO adsorbed after outgassing at $-90\,^\circ C$.

Fig. 8. FT-IR spectra of unreduced Pt-K/Al_2O_3 at $-140\,^\circ C$ after admission of CO gas into the cell until saturation (A) and upon outgassing at increasing temperatures from -140 to $-90\,^\circ C$ (B). In the inserts: (C) OH stretching region of unreduced Pt-K/Al_2O_3 at $-140\,^\circ C$ before and after saturation with CO, and the corresponding difference (after saturation – before saturation); (D) the spectrum of CO adsorbed just after admission (lowest coverage); (E) the spectrum of residual CO adsorbed after outgassing at $-90\,^\circ C$.

reduced a large part of cationic Pt. The carbonyls on zerovalent Pt are evident but the maximum is at a definitely higher frequency ($2098\,cm^{-1}$), suggesting that larger metal particles are formed by reduction. However, the band is large with components at lower frequency suggesting a large distribution of particle size. On the other hand, in agreement with the well-known preference of CO adsorbed over metallic Pt for on-top position, due to electronic factors [31], we do not find evidence of bands of bridging species, in fact usually not observed or extremely small in low loading Pt-Al_2O_3 [30,32].

In Fig. 7 the spectra of CO adsorbed on Al_2O_3, unreduced Pt/Al_2O_3 and reduced Pt/Al_2O_3 and their deconvolutions are reported. The deconvolution of the spectrum of CO adsorbed on alumina allows to only separate the component due to CO interacting with Al^{3+}, found at $2183\,cm^{-1}$, from that due to CO H-bonded on OHs, found at $2152\,cm^{-1}$. In the case of the spectrum of CO adsorbed on unreduced Pt/Al_2O_3 the higher frequency band increases in intensity and shifts up to $2186\,cm^{-1}$, the most intense band shifts up a little bit to $2155\,cm^{-1}$ while a new absorption appears clearly centered at $2135\,cm^{-1}$. In the case of reduced Pt/Al_2O_3 the higher frequency band shifts back down to $2183\,cm^{-1}$ and decreases in intensity, the most intense band shifts also back to $2153\,cm^{-1}$, while the new absorption increases in intensity and shifts up to $2139\,cm^{-1}$.
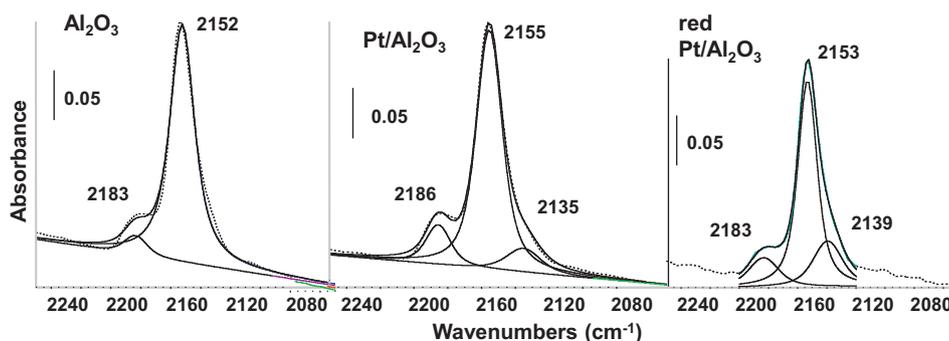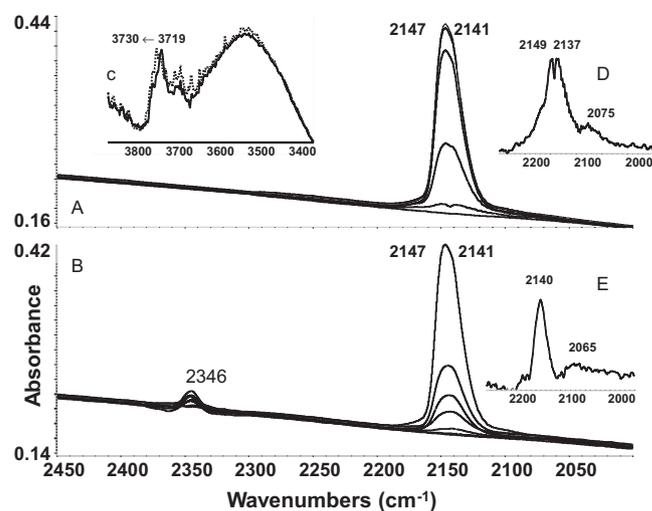
These data suggest that highly oxidized and oxidizing Pt ions contribute to the band at $2186\,cm^{-1}$, and are reduced in the reduced sample. We assign the band at $2186\,cm^{-1}$ predominantly to Pt^{n+}–CO (with $n = 4$ or 2). The band at 2135–$2139\,cm^{-1}$ should be assigned to another form of Pt^{n+}–CO, less oxidized and less oxidant, with $n = 2$ or 1. The amount of the latter species should increase by reduction of the former one. These assignments are consistent with data arising from different authors (reviewed in Ref. [20]) as well as with a previous study from one of our laboratories [17].

In Figs. 8 and 9 the spectra of carbon monoxide adsorbed on the Pt-K/Al_2O_3 catalyst unreduced and reduced, respectively, are reported. At the highest coverage the spectrum is dominated by the band assigned to carbonyl species on K^+ centers. In this case, as for the experiment done with K/Al_2O_3, this band is evidently split into two partially resolved components, as shown by the deconvolutions reported in Fig. 4, located at 2149–2150 and near 2139–$2140\,cm^{-1}$. It seems that the intensity of the higher frequency components increases for the unreduced Pt-K/Al_2O_3 sample with respect to K/Al_2O_3, but decreases back for reduced Pt-K/Al_2O_3. Maybe carbonyls of cationic Pt may contribute to the higher frequency component here. In any case the quality of the two K^+ sites is fully unchanged as an effect of the presence of small amounts of platinum. Also in these cases, like for K/Al_2O_3, the adsorption of CO does not result in any direct interaction with surface OHs. In fact the only perturbation of the OH stretching band
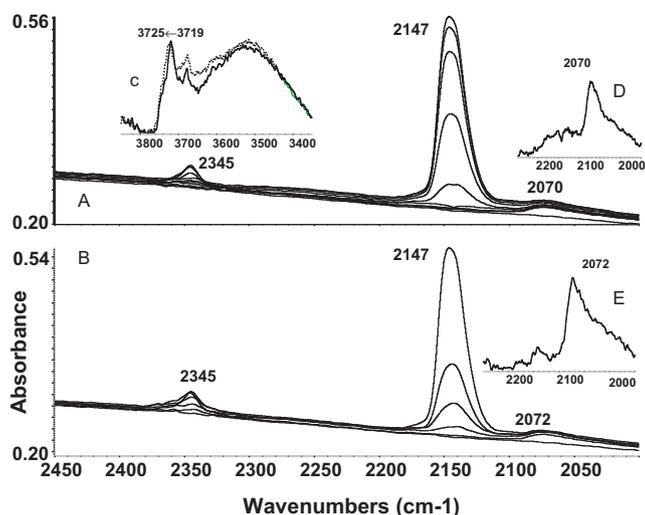

Fig. 7. FT-IR spectra of CO adsorbed on Al_2O_3, on unreduced and prereduced Pt/Al_2O_3 at $-140\,^\circ C$ at saturation (pointed lines), and deconvolution of the spectra.

Fig. 9. FT-IR spectra of prereduced $Pt-K/Al_2O_3$ at $-140\,°C$ after admission of CO gas into the cell until saturation (A) and upon outgassing at increasing temperatures from -140 to $-90\,°C$ (B). In the inserts: (C) OH stretching region of prereduced $Pt-K/Al_2O_3$ at $-140\,°C$ before and after saturation with CO, and the corresponding difference (after saturation – before saturation); (D) the spectrum of CO adsorbed just after admission (lowest coverage); (E) the spectrum of residual CO adsorbed after outgassing at $-90\,°C$.

Fig. 10. FT-IR spectra of CO adsorbed on unreduced and prereduced $Pt-K/Al_2O_3$ at $-140\,°C$ at saturation, and subtraction of the spectra.

consists in a very slight shift up of the band observed at $3719\,cm^{-1}$. This confirms that, at these high K loading levels, surface OHs exist but do not show any Brønsted acidity.

The presence of reduced zerovalent Pt centers is evident on the unreduced $Pt-K/Al_2O_3$ sample, due to the presence of a broad band of carbonyl species at $2075–2065\,cm^{-1}$. The lower frequency observed for these $Pt°$ carbonyls with respect to those observed on Pt/Al_2O_3 is likely due to the effect of the increased basicity of the neighbouring [33]. On the other hand, reductions seem to give rise to better defined Pt particles, where CO adsorbs on-top producing a sharp maximum at $2072\,cm^{-1}$ with a tail at lower frequencies.

In this experiment the oxidation of CO to CO_2 is more limited than on the K-free catalyst, but is not much affected by pre-reduction, suggesting that Pt is more reduced already in the unreduced sample. This may be associated to a higher reactivity of Pt cations as an effect of the presence of potassium, that consequently reduces by decomposition already during outgassing at $350\,°C$. To reveal whether CO adsorption is able to detect unreduced Pt centers on $Pt-K/Al_2O_3$ sample, we analyzed the subtraction spectra of CO adsorbed on reduced and unreduced sample (Fig. 10) after outgassing at $-130\,°C$. While the absorption of CO on metallic Pt is well evident only on the reduced sample, as expected indeed, and appears as a negative peak in the subtraction, in the higher frequency region a small peak at $2150\,cm^{-1}$ is evident as a positive peak, together with an even smaller feature near $2120\,cm^{-1}$. It is possible that these very weak bands arise from Pt^{n+}–CO species over the unreduced sample, although a small perturbation of the K^+–CO band could also be responsible for them.

The spectra we report in Fig. 9 are well different with respect to those reported in the literature for CO adsorption on similar catalysts [34–36], which have, however, been recorded at r.t. To compare better with spectra reported in the literature, we also performed experiments of CO adsorption at room temperature. The spectrum obtained on reduced $Pt-K/Al_2O_3$ sample, after room temperature adsorption of CO and short room temperature outgassing is reported in Fig. 11a. The band due to CO interacting with K^+ ions as well as with Al^{3+} and Pt^{n+} ions (i.e. at $\nu CO > 2100\,cm^{-1}$) cannot be observed at r.t., as indeed expected to the weakness of these interactions which are only detectable at low temperature. However, a
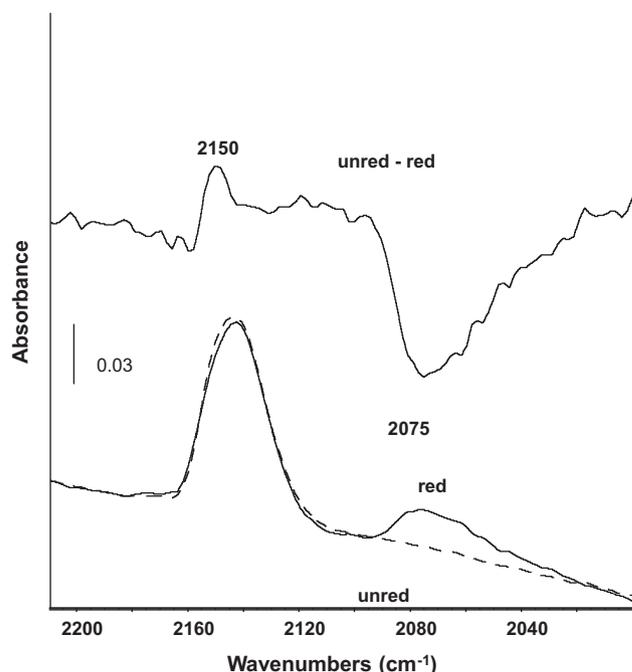
stronger band is observed in the field of terminal carbonyls on platinum, centred at $2056\,cm^{-1}$, with a prominent shoulder centred at $2008\,cm^{-1}$, while an additional band is found at $1800\,cm^{-1}$, in the typical region of bridging carbonyls. Additionally, also very strong bands are observed at 1580 and $1332\,cm^{-1}$, that should be assigned to carbonate ions, which are observed much weaker at low temperature, in parallel to the formation of CO_2. The spectrum we observe in these conditions is similar to those reported by other authors at room or higher temperatures, on similar catalysts. Derrouiche et al. [34] with a 2.9% $Pt-10\%K-Al_2O_3$ catalyst observe at room and higher temperatures bands at 2050, 1950 and $1763\,cm^{-1}$, assigned to linear and bridging CO on $Pt°$, and species adsorbed on a Pt-K site, respectively. Prinetto et al. [35,36] at room temperature find a similar spectrum, with a band in the region $2045–2015\,cm^{-1}$ assigned to on-top carbonyls on $Pt°$, a band at $1945–1955\,cm^{-1}$, of uncertain assignment, and a third band at $1735–1690\,cm^{-1}$, assigned to bridging carbonyls. In fact the experiments of CO adsorption at
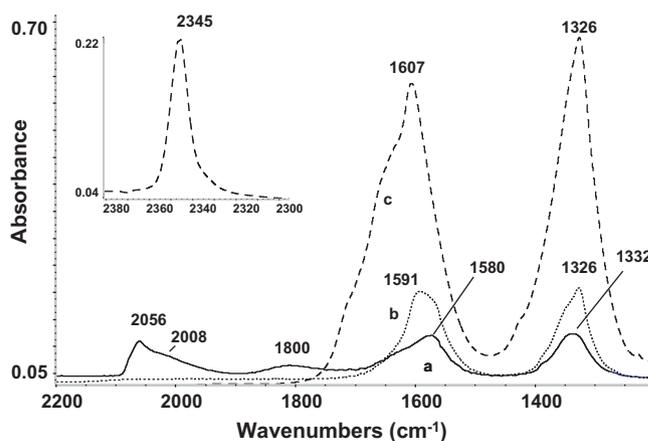

Fig. 11. FT-IR spectra of CO adsorbed on prereduced $Pt-K/Al_2O_3$ at r.t. (a) and after outgassing at $100\,°C$ (b), and spectrum of CO_2 adsorbed on prereduced $Pt-K/Al_2O_3$ at r.t. (c).
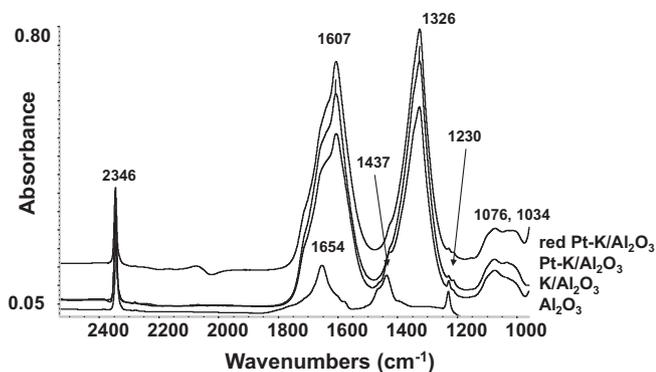
Fig. 12. FT-IR spectra of CO_2 adsorbed on Al_2O_3, K/Al_2O_3 and unreduced and prereduced Pt-K/Al_2O_3 at r.t. at saturation.

Fig. 13. TPD curves of CO_2 from Pt/Al_2O_3 and Pt-K/Al_2O_3.

room or higher temperatures are affected by the reactivity of CO itself, that produces also relevant amounts of carbonate species and CO_2, and perhaps undetectable carbide species, that likely modify the state of the surface and may be also responsible for the band in the 1800–1700 cm^{-1} region [37] previously assigned to bridging CO. Other works report that bridging carbonyls on Pt absorb in the 1950–1850 cm^{-1} range on both low index faces [38] and on stepped surfaces [39]. In an early work [25] it has been reported that CO adsorption on 12% wt/wt K_2CO_3-Al_2O_3 catalyst does not give rise to any carbonyl formation but produces (in the absence of oxidizing agents) further carbonates, like observed here for Pt-K/Al_2O_3, confirming some kind of Boudouard-like reactivity.

Interestingly, upon outgassing at 100 °C (Fig. 11b) the bands of carbonate species even grow, likely due to the further oxidation of CO by unreduced Pt centers. The spectra of carbonate species are in similar (although not identical) positions as those observed upon adsorption of carbon dioxide over the same reduced surface (Fig. 11c).

Low temperature adsorption experiments allow the observation of weakly acidic but very active sites like K$^+$, not observed in room or higher temperature experiments, but also to avoid excessive reactivity of CO, finally giving a more precise picture of the state of the surface. However, room temperature experiments may perhaps provide evidence for some kind of "activated" adsorption phenomena, allowing several kinds of different adsorption modes needing some energy to be allowed. The spectra observed after adsorption of CO on the Pt-K/Al_2O_3 catalyst, in analogy with those reported recently for Pt-Na/TiO_2 catalysts [40], show the shift down of the absorption due to terminal carbonyls and the increased formation of bridging species caused by the addition of potassium. This could be interpreted as a further evidence of the increased electrondonating character of Pt metal centers when potassium is copresent. However, the difference among the spectra recorded at low and room temperature is indicative of more complex interactions occurring at room temperature that need some activation energy to be established. We suggest the occurrence, only upon adsorption at sufficiently high temperatures (room and higher), of complex interactions similar to those occurring on some deeply cation exchanged alkali zeolites such as Na-, K- and Cs-ferrierite [41]. In this case, in addition of the normal C-bonding of CO to metal centers, additional interaction occurs either through the oxygen lone pairs or through the π-type orbitals, leading to a lowering of CO stretching frequency. We tentatively suggest that some kind of additional interaction of Pd°-carbonyls with K$^+$ cations may be established on Pt-K/Al_2O_3 catalyst only at room or higher temperatures.
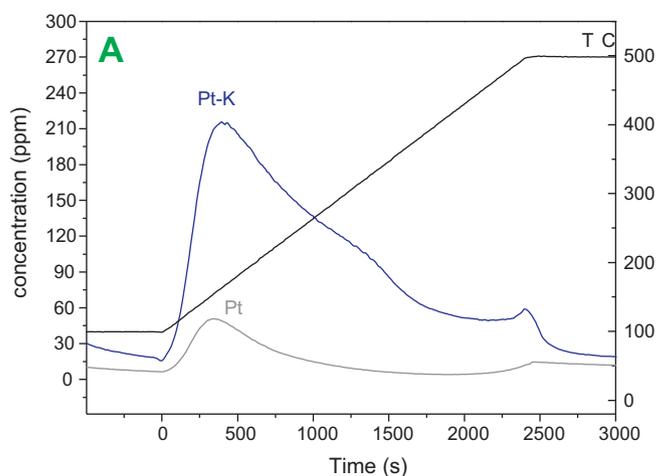
3.3. IR spectra of adsorption of CO_2 adsorption and CO/CO_2 coadsorption

In Fig. 12 the IR spectra obtained after CO_2 adsorption on Al_2O_3, on K/Al_2O_3 and on unreduced and reduced Pt-K/Al_2O_3 are compared. The spectra obtained on K/Al_2O_3 and both reduced and unreduced Pt-K/Al_2O_3 are almost identical, being dominated by features typical of bridging or bidentate carbonates (main features at 1607, 1326 and 1076 cm^{-1} [42], in contrast to the bands at 3618 (not shown), 1654, 1437 and 1230 cm^{-1}), due to surface bicarbonate species. These data confirm the significant basicity (or acidobasicity) induced by potassium that totally transforms at these loading levels the acidobasicity of alumina. This is also evident from the CO_2-TPD curves shown in Fig. 13. While CO_2 desorption from Pt/Al_2O_3 is complete already at 200 °C, to have an almost complete desorption from Pt-K/Al_2O_3 350 °C are needed with a small desorption of CO_2 also at 500 °C. Also the amount of CO_2 desorbed from Pt-K/Al_2O_3 is more than 5 times that desorbed from Pt/Al_2O_3.

To have a further indication on the role of K-Pt interactions, we performed an experiment of sequential adsorption of CO_2 and CO over the reduced Pt-K/Al_2O_3 catalyst. In Fig. 14a, the spectrum of the reduced Pt-K/Al_2O_3 is reported. We note that the sample shows two very weak absorptions at 1562 and 1355 cm^{-1} which can be assigned to carboxylate/carbonate impurities arising from
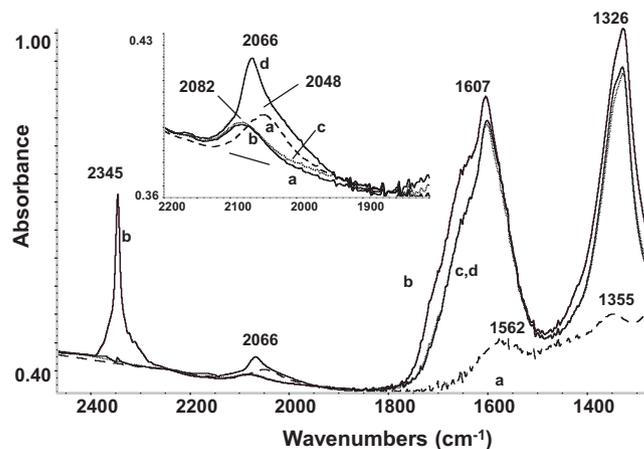

Fig. 14. FT-IR spectra of activated prereduced Pt-K/Al_2O_3 at room temperature (a), after adsorption of CO_2 (b), after outgassing at r.t. (c) and after successive adsorption of CO (d).
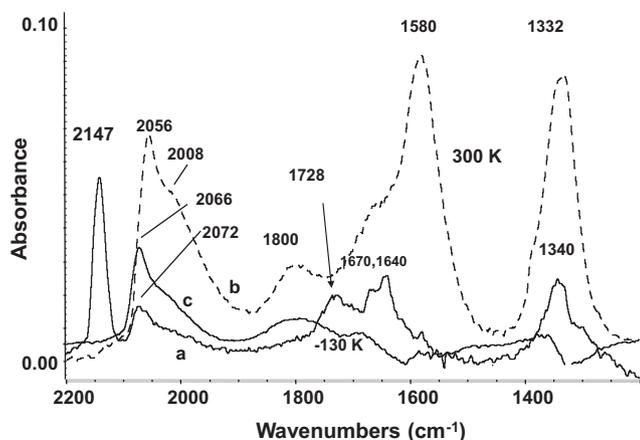
Fig. 15. Comparison of the FT-IR spectra of CO adsorbed on prereduced Pt-K/Al$_2$O$_3$ at $-140\,^\circ$C (a) and at room temperature (b), and over CO$_2$-precovered prereduced Pt-K/Al$_2$O$_3$ at room temperature (c).

chemicals used in the preparation (e.g. acetate ions used in potassium impregnation). Additionally the spectrum shows a residual weak band at 2048 cm^{-1} (Fig. 14a), which may be attributed to CO stretching of Pt carbonyl species, that probably also origin from the conversion of chemicals used in the preparation. The frequency observed is in the same range as that observed in the experiment of CO adsorption at r.t. in Fig. 11. Adsorption of carbon dioxide causes, as said, the formation of the bands of carbonates (main maxima at 1607 and 1326 cm^{-1}) and linearly adsorbed CO$_2$ (2345 cm^{-1}). Additionally, the shift up to 2082 cm^{-1} of the band previously observed at 2048 cm^{-1} is also evident (Fig. 14b). The band resists in this position also after outgassing at r.t. (Fig. 14c), that causes the disappearance of molecularly adsorbed CO$_2$ but leaves bridging carbonates on the surface. This indicates that Pt species responsible for the strongest adsorption of CO is sensitive to the presence of carbonate species, thus being very likely located near the basic sites where carbonates form. Further additional contact with CO produces a new maximum now at 2066 cm^{-1}. As shown by the comparison reported in Fig. 15, the spectrum observed after CO adsorption on the "carbonate precovered" reduced surface is very similar (in the 2200–1800 cm^{-1} region) to that observed after CO adsorption on the clean reduced surface, but definitely less intense. The main maximum is observed at 2066 cm^{-1} (Fig. 15c), i.e. at an intermediate position between those observed on the reduced surface at room (2056 cm^{-1}, Fig. 15b) and at low temperature (2072 cm^{-1}, Fig. 15a). These data indicate that Pt centers should lie in close proximity of potassium oxides generating basicity. In fact part of Pt sites seem to be "poisoned" by carbonate species formed on K oxide centers, while part of them are perturbed electronically by the presence of such species, thus showing higher CO stretching frequencies.

4. Conclusions

The data discussed above allow us to draw the following conclusions.

1. Platinum in small amounts on alumina does not affect the number and the strength of Lewis acid sites of hydroxylated alumina. This suggests that Pt atoms tend to locate over basic sites of alumina.
2. Unreduced Pt deposed on alumina upon outgassing at 350 $^\circ$C gives rise to at least three different species: i) highly oxidizing Pt cations (Pt^{4+} or Pt^{2+}), whose carbonyls are found at 2186 cm^{-1}; ii) less oxidizing Pt cations (Pt^{2+} or Pt$^+$) whose carbonyls are found

at 2135–39 cm^{-1}; iii) well dispersed reduced zerovalent Pt particles whose carbonyls are found at 2085 cm^{-1}. Highly oxidizing Pt cations are so active to oxidize CO to CO$_2$ at 150 K.
3. Mild reduction in our condition reduced highly oxidizing Pt cations to the less active cationic species and perhaps to the zerovalent state. In any case, zerovalent Pt tends to coalesce to give rise to larger particles characterized by CO of carbonyl species at 2098 cm^{-1}. No bridging carbonyl species are found in these conditions.
4. The presence of K in Pt-K/Al$_2$O$_3$ catalysts seems to increase the reducibility of Pt, whose highly oxidizing species are not observed after outgassing at 350 $^\circ$C. Additionally, the basicity of K/Al$_2$O$_3$ increases the electron density on reduced Pt, as evidenced by the slightly lower CO stretching frequency of Pt carbonyls.
5. The comparison of the data obtained upon low temperature adsorption of CO with those obtained by adsorption at room temperature show that CO acts, at room temperature, not as a completely inert probe. In fact, the formation of carbonates without any oxidant (except Pt species, in case) and the relevant modification of the spectrum of adsorbed CO suggest some reactivity of CO at r.t. On the other hand, already at $-100\,^\circ$C CO reduces a small part of the surface Pt ions producing CO$_2$. This makes low-temperature CO adsorption experiments an informative tool for the surface characterization.
6. Pt species are located near the basic oxide species of the K/Al$_2$O$_3$ "support" and their behavior is influenced by the presence of adsorbed carbonate species.

References

[1] R.S. Haizmann, L.H. Rice, M.S. Turowicz, US patent 5453552 (1995) to UOP.
[2] M.M. Bhasin, J.H. McCain, B.V. Vora, T. Imai, P.R. Pujadó, Appl. Catal. A: Gen. 221 (2001) 397.
[3] D.R. Dyroff, U.S. Patent No. 6,700,028 B2, to Huntsmann Petrochem. Co. (2004).
[4] A.A. Phatak, N. Koryabkina, S. Rai, W. Ruettinger, R.J. Farrauto, G.E. Blau, W.N. Delgass, F.H. Ribeiro, Catal. Today 123 (2007) 224–234.
[5] M. Garcia-Diéguez, E. Finocchio, M.A. Larrubia, L.J. Alemany, G. Busca, J. Catal. 274 (2010) 11–20.
[6] Y. Choi, H.G. Stenger, J. Power Sources 129 (2004) 246–254.
[7] H. Tanaka, M. Kuriyama, Y. Ishida, S. Ito, K. Tomishige, K. Kunimori, Appl. Catal. A: Gen. 343 (2008) 117–124.
[8] P. Harrison Tran, J.M.H. Chen, G.D. Lapadula, T. Blute, US patent 7410626 B2 (2008) to BASF Catalysts LLC.
[9] P. Hurtado, S. Ordóñez, A. Vega, F. Diez, Chemosphere 55 (2004) 681–689.
[10] G. Avgouropoulos, E. Oikonomopoulos, D. Kanistras, T. Ioannides, Appl. Catal. B: Environ. 65 (2006) 62.
[11] G. Busca, Ind. Eng. Chem. Res. 48 (2009) 6486.
[12] W.S. Epling, L.E. Campbell, A. Yezerets, N.W. Currier, J.E. Parks II, Catal. Rev. 46 (2004) 163.
[13] N. Takahashi, H. Shinjoh, T. Iljima, T. Suzuki, K. Yamazaki, K. Yokota, H. Suzuki, N. Miyoshi, S. Matsumoto, T. Tanizawa, T. Tanaka, S. Tateishi, K. Kasahara, Catal. Today 27 (1996) 63.
[14] K. Nakatani, S. Hirota, S. Takeshima, K. Itoh, T. Tanaka, SAE Paper SP-1674 (2002) 2002-01-0957.
[15] I.S. Pieta, M. Garcia Diguez, C. Herrera, M.A. Larrubia, L.J. Alemany, J. Catal. 270 (2010) 256–267.
[16] M.R. Lee, E.R. Allen, J.T. Wolan, G.B. Hoflund, Ind. Eng. Chem. Res. 37 (1998) 3375.
[17] I. Malpartida, M.A. Larrubia Vargas, L.J. Alemany, E. Finocchio, G. Busca, Appl. Catal. B: Environ. 80 (2008) 214–225.
[18] J.H. Kwak, J. Hu, D. Mei, C.-W. Yi, D.H. Kim, C.H.F. Peden, L.F. Allard, J. Szanyi, Science 325 (2009) 1670–1673.
[19] H. Knözinger, S. Huber, J. Chem. Soc., Faraday Trans. 94 (1998) 2047.
[20] K.I. Hadjiivanov, G.N. Vayssilov, Adv. Catal. 47 (2002) 307.
[21] G. Busca, in: S.D. Jackson, J.S.J. Hargreaves (Eds.), Metal Oxide Catalysis, vol. 1, Wiley-VCH, 2008, p. 95.
[22] V. Sanchez-Escribano, L. Arrighi, P. Riani, R. Marazza, G. Busca, Langmuir 22 (2006) 9214.

[23] E. Finocchio, G. Busca, P. Forzatti, G. Groppi, A. Beretta, Langmuir 23 (2007) 10419.
[24] S. Specchia, E. Finocchio, G. Busca, P. Palmisano, V. Specchia, J. Catal. 263 (2009) 134.
[25] M. Kantschewa, E.V. Albano, G. Ertl, H. Knözinger, Appl. Catal. 8 (1983) 71.
[26] G. Busca, V. Lorenzelli, G. Ramis, R. Willey, Langmuir 9 (1993) 1492.
[27] P.O. Scokart, A. Amin, C. Defosse, P.G. Rouxhet, J. Phys. Chem. 85 (1981) 1406.
[28] G. Busca, G. Ramis, Appl. Surf. Sci. 27 (1986) 114–126.
[29] T. Montanari, I. Salla, G. Busca, Micropor. Mesopor. Mater. 109 (2008) 216–222.
[30] L.-C. De Ménorval, A. Chaqroune, B. Coq, F. Figueras, J. Chem. Soc., Faraday Trans. 93 (1997) 3715.
[31] C. Hippe, R. Lambert, G. Schultz-Ekloff, U. Schubert, Catal. Lett. 43 (1997) 195.
[32] J. Raskò, J. Catal. 217 (2003) 478.
[33] S. Albertazzi, G. Busca, E. Finocchio, R. Glöckler, A. Vaccari, J. Catal. 223 (2004) 372.

[34] S. Derrouiche, P. Gravejat, B. Bassou, D. Bianchi, Appl. Surf. Sci. 253 (2007) 5894.
[35] L. Castoldi, L. Lietti, I. Nova, R. Matarrese, P. Forzatti, F. Vindigni, S. Morandi, F. Prinetto, G. Ghiotti, Chem. Eng. J. 161 (2010) 416.
[36] F. Prinetto, M. Manzoli, S. Morandi, F. Frola, G. Ghiotti, L. Castoldi, L. Lietti, P. Forzatti, J. Phys. Chem. C 114 (2010) 1127.
[37] G. Ramis, G. Busca, V. Lorenzelli, Mater. Chem. Phys. 29 (1991) 425–435.
[38] D. Curulla, A. Clotet, J.M. Ricart, F. Illas, J. Phys. Chem. 103 (1999) 5246.
[39] J. Xu, J.T. Yates, Surf. Sci. 327 (1995) 193.
[40] P. Panagiotopoulou, D.I. Kondarides, J. Catal. 260 (2008) 141.
[41] I. Salla, T. Montanari, P. Salagre, Y. Cesteros, G. Busca, Phys. Chem. Chem. Phys. 7 (2005) 2526.
[42] G. Busca, V. Lorenzelli, Mater. Chem. 7 (1982) 89.